

# Application of 2D full-wave simulations to study plasma turbulence with conventional reflectometry<sup>a</sup>

J. Vicente,<sup>1b</sup> F. da Silva,<sup>1</sup> S. Heuraux,<sup>2</sup> G.D. Conway<sup>3</sup>, C. Silva,<sup>1</sup> and T. Ribeiro<sup>3</sup>

<sup>1</sup>*Instituto de Plasmas e Fusão Nuclear, Instituto Superior Técnico, Universidade de Lisboa, 1049-001 Lisboa, Portugal*

<sup>2</sup>*Institut Jean Lamour, UMR 7198 CNRS-University of Lorraine, F-54506 Vandoeuvre, France*

<sup>3</sup>*Max-Planck-Institut für Plasmaphysik, 85748 Garching, Germany*

A well established two-dimensional (2D) finite-difference time-domain (FDTD) full-wave code (REFMUL) has been used to perform conventional reflectometry simulations on broadband turbulent numerical plasmas. Probing with fixed frequency O-mode polarized waves was employed together with *In-phase* and *Quadrature (IQ)* detection to obtain phase  $\varphi(t)$  and amplitude  $A(t)$  measurements. The plasma electron density was modeled following a Kolgomorov-like amplitude  $k$ -spectrum and the turbulence level  $\delta n_e/n_e$  of the electron density was scanned in sets of simulations where a bulk plasma flow was forced in either the radial or the poloidal direction. Results show spectral broadening of the complex reflectometry amplitude signals with increasing turbulence levels. Simulations also show that phase variations are proportional to turbulence levels, only in cases of low turbulence levels, as previously observed with 1D and 2D physical optics codes. The onset of non-linear effects in the phase response was observed and associated with phase jumps and phase runaway occurring above certain turbulence levels in both cases of poloidal and radial plasma flow.

## I. Introduction

The problem of interpreting reflectometry measurements and inferring turbulence characteristics from fusion plasmas probed with microwave beams remains complex. Full-wave simulations have been instrumental in understanding different scattering mechanisms, such as *Bragg backscattering* or *forward scattering* [1]. However, the conditions for reflectometry at nuclear fusion devices are usually far away from linear response regimes where reflectometry interpretation is straightforward. Reflectometry

---

<sup>a</sup> Contributed paper, published as part of the Proceedings of the 13<sup>th</sup> International Reflectometry Workshop, Daejeon, South Korea, May 2017

<sup>b</sup> jvicente@tecnico.ulisboa.pt

simulations using realistic plasma models is a continuous effort that must be pursued as increasing computational power and more sophisticated plasma models are available.

## II. The Simulation Setup

The full-wave code REFMUL used in this work solves the Maxwell equations for ordinary wave polarization (O-mode). Both electric and magnetic fields are coupled to the plasma electron density  $n_e(\mathbf{r}, t)$  which is used to model the fusion plasma [2]. The simulation box comprises a rectangular grid with Cartesian dimensions  $L_x$  and  $L_y$  corresponding to the radial and poloidal directions in the usual tokamak coordinates. In this work, typically  $L_x = 40\text{cm}$  while the plasma itself has a smaller radial extent ( $\approx 15\text{cm}$ ) since part of the simulation box is used for the antenna setup and a vacuum distance to the plasma. The time duration of any simulated phenomena has to be scaled down, and any velocities involved scaled up. Consider a plasma feature with characteristic dimension  $L_p$  moving with velocity  $v_{\text{real}}$ . In the simulation, the velocity  $v_{\text{siml}}$  will be set by the time  $t_{\text{sml}}$  that the same plasma feature will take to pass a given point, i.e.  $v_{\text{siml}} = L_p / t_{\text{sml}}$ . Hence, a rescaling is done such that  $v_{\text{siml}} = R_t v_{\text{real}}$ . In addition, to avoid relativistic effects the resulting scaled-up velocities  $v_{\text{siml}}$  are restricted to values of  $v_{\text{siml}} < 0.1c$ , where  $c$  is the speed of light. Using typical values employed in this work ( $L_p = 2000$  grid points, and  $t_{\text{sml}} = 100000$  time iterations with time step  $\Delta t = 6.25 \times 10^{-13}\text{s}$ ), the velocity ratio obtained is of the order of  $R_t = 1200$ .

Simulations were designed with a monostatic setup, i.e. one antenna for both emission and reception. A unidirectional transparent source was used for injection of the signal allowing separating the emitted probing wave from any returning waves. For directivity a monostatic 2D H-plane horn antenna was used with a half-power beam width of  $\approx 6.5\text{cm}$  at the plasma entry. The probing wave was selected with frequency  $f_o = 33\text{GHz}$  and wavelength in vacuum  $\lambda_o \approx 0.9\text{cm}$ , corresponding to a cutoff density  $n_c = 1.35 \times 10^{19}\text{m}^{-3}$ . Finally, the reflectometry phase and amplitude signals were obtained using an  $IQ$

detection method that provides  $I(t) = A(t) \cos \varphi(t)$  and  $Q(t) = A(t) \sin \varphi(t)$  signals, which combined give amplitude and phase signals:

$$A(t) = \left( I^2(t) + Q^2(t) \right)^{1/2}, \quad \varphi(t) = \arctan \left( \frac{Q(t)}{I(t)} \right). \quad (1), (2).$$

The characteristics of the antenna, the wave emission, and detection scheme have been chosen taking into account what can be found in typical plasma edge studies carried out with a conventional reflectometry system at the ASDEX Upgrade tokamak [3].

### III. Plasma Turbulence Model

The plasma in O-mode simulations is uniquely modeled through the definition of the electron density  $n_e(\mathbf{r}, t)$ . A slab unperturbed background plasma with radial linear electron density profile  $n_{eo}$  was first considered. Two different electron density gradient lengths  $L_n$  have been used in this work, corresponding to a shallow ( $L_{n,sh} = 0.169\text{m}$ ) and a steep ( $L_{n,st} = 0.0176\text{m}$ ) density profile. These gradient lengths, equivalently referred in unit of grid points in following sections as  $l_c=213$  and  $l_c=640$ , respectively, are comparable to those found in L-mode discharges at the ASDEX Upgrade tokamak, for example during low and high fuelling periods. Broadband plasma turbulence was also included calculating a turbulence term  $\delta n_e$  which is added to  $n_{eo}$ , such that the total electron density is given by  $n_e(\mathbf{r}, t) = n_{eo}(\mathbf{r}, t) + \delta n_e(\mathbf{r}, t)$ . While the background profile is set through the electron density gradient, the turbulence matrix is defined using a given model. The turbulence model employed here is given by a sum of modes with random phase, as in [4,5]:

$$\delta n_e = \sum_{i=i_m}^{i_M} \sum_{j=j_m}^{j_M} A(i, j) \cos[k_x(i)x + k_y(j)y + \varphi(i, j)]. \quad (3)$$

The coefficients  $A(i, j)$  establish an amplitude spectrum (which can be chosen to be Gaussian, Uniform, Kolgomorov, etc.) and  $\varphi(i, j)$  is a random generated phase which sets a particular turbulence *snapshot* (or realization) from an infinite set of possibilities sharing the same spectral conditions. In this

work, a Kolgomorov-like amplitude  $k$ -spectrum was used which is in line with several turbulence observations in the edge plasmas of experimental fusion reactors. This  $k$ -spectrum is defined by a constant amplitude up to a chosen wavenumber  $k_{knee}$  (rad/m) followed by a power law  $k_f^{-3}$  decay along both the radial and the poloidal directions. The wavenumber  $knee$  was set to  $k_{knee} = 400$  rad/m , or  $k_{knee} = 4\text{cm}^{-1}$  in usual units which corresponds to a wavelength of  $\lambda_{knee} = 16\text{cm}$ . The amplitude drops to 1% of the flat top value at 1500 rad/m. The finite dimensions of the simulation box and the spatial grid spacing ( $\Delta x = \Delta y$ ) set the minimum and maximum wavenumbers, respectively, that can be resolved. A minimum wavelength of 2 spatial steps ( $\Delta x = \Delta y = 3.75 \times 10^{-4}\text{m}$ ), sets  $k_{Max} = 84\text{cm}^{-1}$  in both the  $x$ -direction and the  $y$ -direction while  $k_{x, Min} = 0.42\text{cm}^{-1}$  (using  $L_x = 15\text{cm}$  as maximum wavelength value) and  $k_{y, Min} = 0.084\text{cm}^{-1}$  (using  $L_y = 75\text{ cm}$ ).

The turbulence level usually referred as  $\delta n_e/n_e$  has been set using:

$$\frac{\delta n_{e,RMS}}{n_e(x_c)} \times 100\% , \quad (4)$$

where  $\delta n_{e,RMS}$  is the Root Mean Square (RMS) value of the density fluctuations, and  $x_c$  the radial position of the cutoff density in the slab linear profile. After generating a turbulence matrix, using the previously presented model, a multiplication factor can thus be used to change the RMS of the matrix and consequently the turbulence level. This way, adding the density turbulence term to the linear profile results in a radial variation of the actual turbulence level, which increases towards the periphery of the plasma as the background density decreases. This kind of radial trend for the turbulence level is reasonable when considering the edge and SOL regions of experimental plasmas in tokamaks.

Reflectometry simulations are carried out with the total density matrix (plasma) moving either in the  $y$ -direction or in the  $x$ -direction, corresponding to the poloidal and radial directions in a tokamak, respectively. In any case, the Taylor “frozen turbulence” hypothesis is assumed, which considers that advection contribution by turbulent eddies is small and that therefore the advection past a fixed point can

be taken to be entirely due to the mean flow. This hypothesis holds if the relative turbulence intensity is small, i.e. for  $u \ll U$ , where  $u$  is the eddy velocity and  $U$  is the mean plasma velocity.

#### IV. Bragg Backscattering

It has been shown that reflectometry phase variations are mainly due to backscattering of the incident wave by density fluctuations that meet the Bragg resonant rule [6,7,8]. For conventional reflectometry, the poloidal characteristics of density perturbations should not be responsible for any backscattering (although in 2D it is impossible to neglect the radiation pattern of the emitter which contains poloidal wavenumbers and thus could resonate with poloidal fluctuations) but Bragg backscattering can certainly occur when the local radial wavenumber of the injected wave  $k(\mathbf{r})$  is resonant with  $k_{rad}$ , the radial turbulence wavenumber:  $k_{rad} = 2k(\mathbf{r})$  [9]. However, density structures of very small wavenumber do not originate resonant scattering and the response is localized at the cut-off. Only fluctuations with  $k_{rad} > 2k_A$  can satisfy the Bragg condition, where  $k_A$  is the Airy wavenumber:

$$k_A = 0.63(k_o^2 L_n^{-1})^{1/3}. \quad (5)$$

The minimum plasma fluctuation wavenumber allowing Bragg backscattering,  $k_{rad} = 2k_A$ , resonates in the vicinity of the cut-off. Considering the two values of density gradient lengths used in this work and the chosen wave frequency, we obtain the minimum Bragg fluctuation wavenumbers:  $k_{\text{Bragg,sh}} = 1.78\text{cm}^{-1}$ , and  $k_{\text{Bragg,st}} = 3.79\text{cm}^{-1}$ . Therefore, in both cases, the turbulence generated and added to the simulated plasma enables Bragg backscattering to occur. In the case of O-mode probing and small coherent perturbations, a linear relation between the phase perturbations  $\delta\varphi$  and the density perturbation amplitude  $\delta n$  has been predicted [9]:

$$\delta\varphi \propto \left( \frac{L_n}{k_f} \right)^{1/2} \frac{\delta n}{n_c}. \quad (6)$$

For density perturbations of large amplitude, the relation between the reflectometry phase shift and the perturbation amplitude is no longer simple [10]. A strong reflection in a Bragg resonance position might occur, far away from the cut-off, leading to a strong nonlinear regime of Bragg backscattering [11].

## V. Simulation Results

### A. Poloidal Plasma Flow

Simulations with two density gradient lengths ( $l_c=213$  and  $l_c=640$ ) were performed to scan the turbulence level, in cases where a plasma flow in the poloidal direction was imposed. The turbulence level at the cut-off position was varied in the range of 0.02%-20%. In one of the simulation series a fairly steep density profile was used ( $l_c=213$ ) while a shallower linear profile was employed ( $l_c=640$ ) in the second series. In both cases, a constant poloidal velocity  $v_{pol}$  corresponding to 4% of the speed of light was used. Figure 1 shows the power spectra of the reflectometry complex amplitude signal  $A(t)e^{i\varphi(t)}$  for selected values of turbulence levels, in each case of density gradient length.

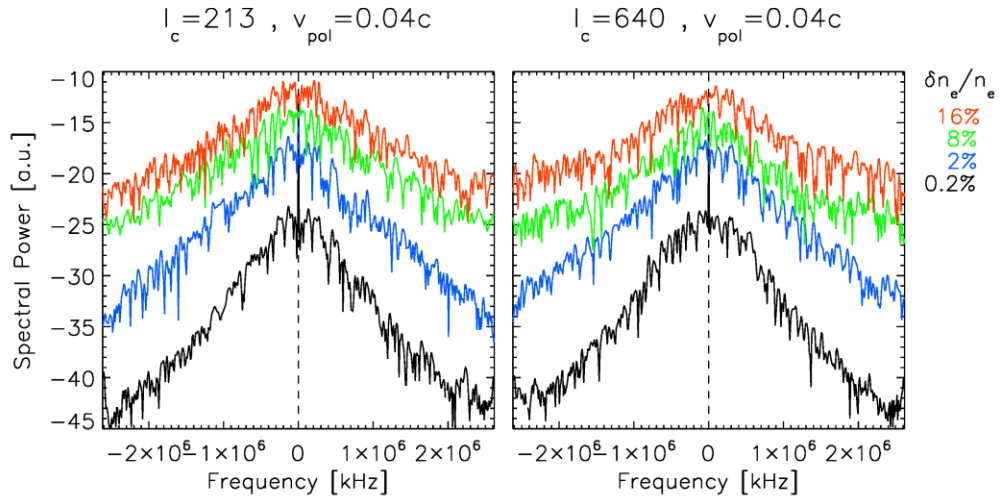


FIG. 1. Power spectra of reflectometry complex amplitude signal  $A(t)e^{i\varphi(t)}$  for a set of chosen turbulence levels, in two different density gradient lengths of background *slab* plasmas. Turbulence was generated using a Kolgomorov-like model and set to flow in the poloidal direction. Spectra are displaced vertically to help visualize the data.

Aside from the spectra obtained at 0.2% turbulence level, all remaining spectra were displaced to help in visualizing the data. On each  $i^{\text{th}}$  turbulence level considered (for the same gradient length), an offset of  $+3i$  a.u. was introduced in the corresponding spectral power. In general, a spectral broadening with increasing turbulence level seems to be observed. The usual increase of central peak amplitudes and integrated spectral powers with increasing turbulence level can also be observed in figure 2, where spectra of the fluctuating components of both amplitude and phase are displayed (e.g. see [4] where similar results were obtained with a physical optics model). In addition, the spectral broadening effect is also observed for increasing turbulence levels.

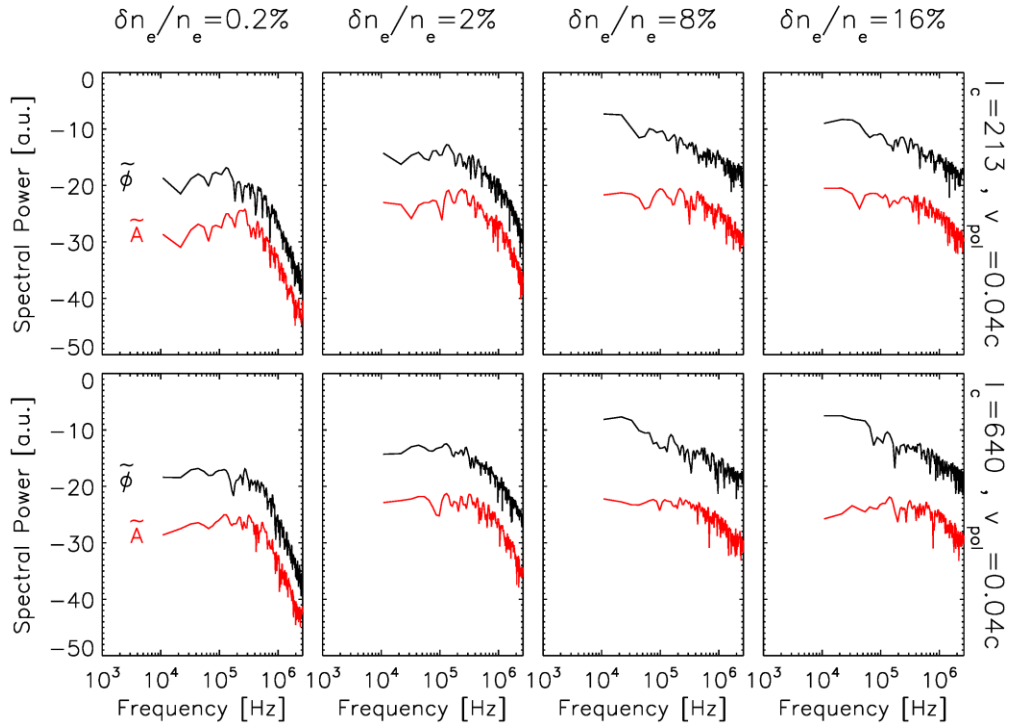


FIG. 2. Power spectra of reflectometry amplitude  $A(t)$  and phase  $\varphi(t)$  signals for the same cases shown in Figure 1.

It is known that fluctuations moving in the poloidal direction, acting as a phase grating, may result in frequency shifted sidebands at the receiver antenna. However, the amplitudes of those sidebands are expected to be equal in conventional reflectometry (i.e. with perpendicular incidence), at least for geometrically symmetric perturbations and typical propagation velocities. On the other hand, the

poloidal propagation of density structures results in a radial displacement of the cutoff layer as the 2D structures project different radial profiles along their movement. It is also commonly observed that the phase response originates mainly from the cutoff layer and fluctuations in its vicinity. Thus, any radial movements of the reflecting layer should lead to a phase modulation of the reflected signal, resulting in a symmetric broadening of the central line in the frequency spectrum. However, Doppler effects in both directions can take place with different efficiency depending on the Bragg resonant position (less efficiently at the plasma edge and more in the vicinity of the cut-off) which will shape the spectra.

It is also observed a spectral broadening effect for increasing density gradient length, at the equivalent turbulence levels. This might be mainly determined by the increasing path length into the plasma [12].

The time evolution of the amplitude  $A(t)$  and phase  $\varphi(t)$  obtained in the cases previously shown are displayed in figure 3.

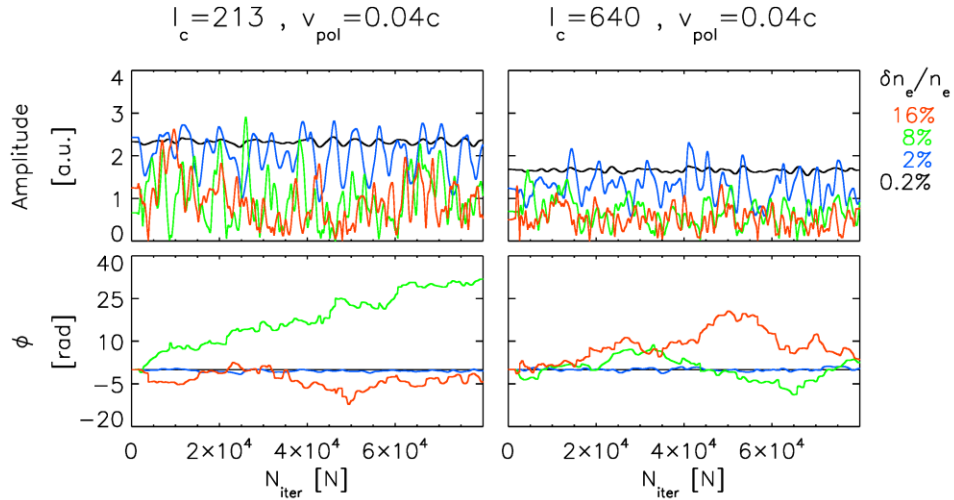


FIG. 3. Evolution of reflectometry amplitude  $A$  and phase  $\varphi$  along the time iterations  $N_{\text{iter}}$  corresponding to poloidal propagation of the turbulence matrix. The simulated cases depicted here are the same shown in figures 1 and 2.

For each density gradient length, the average amplitude of the reflected signal decreases with increasing turbulence level. This is not surprising as loss of coherence in the signal is expected due to



increased scattering. It is also observed that, for each turbulence level, the average amplitude is lower in the case of higher density gradient length. This might also be related with the beam spreading associated to a longer path into the turbulent plasma. The phase behavior shows drifting and phase runaway already at moderate turbulence levels. In figure 4 the standard deviation of both the phase and amplitude signals are displayed for the more comprehensive set of simulations (i.e. turbulence levels) that were studied.

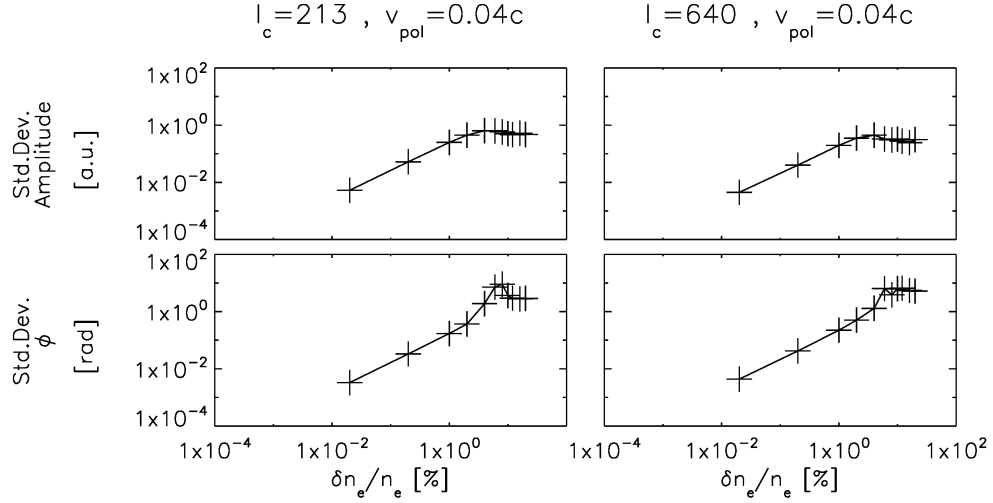


FIG. 4. Standard deviation of the reflectometry amplitude  $A(t)$  and phase  $\varphi(t)$  signals against the turbulence level of the Kolgomorov-like turbulent plasmas for two density gradient length cases, using a log-log plot.

The linear relation between the reflectometry phase and the turbulence level, predicted by equation (6), seems to hold only for very low turbulence levels up to  $\delta n_e/n_e \approx 2\text{-}4\%$  at the cutoff position, which also depends on the square root of the density gradient length. At higher turbulence levels there is a non-linear response that seems to fade into a quasi-saturated regime at the highest turbulence levels. Similar trends are also observed in the amplitude of the reflected signals. The limited range of linear responses from reflectometry phase to plasma turbulence levels has been previously predicted with 2D physical optics models, despite neglecting radial effects such as Bragg backscattering [13]. Using 1D analytical reasoning, where strong Bragg backscattering regimes have been considered, also lead to similar conclusions [11].

## B. Radial Plasma Flow

Simulations were also carried out with the turbulent plasma flowing at constant radial velocity  $v_{\text{rad}}$ , in the direction corresponding to downward propagation along the density profile. The same density matrices were employed as in the previous cases, but  $v_{\text{rad}}$  was 3% of the speed of light, because of the slight difference between the radial and poloidal sizes of the matrix, which is fully swept across the line of sight of the antenna in each corresponding direction of plasma propagation.

The double-sided Fourier spectra of the complex amplitude are presented in figure 5 for both cases of density gradient lengths considered previously and the same set of turbulence levels.

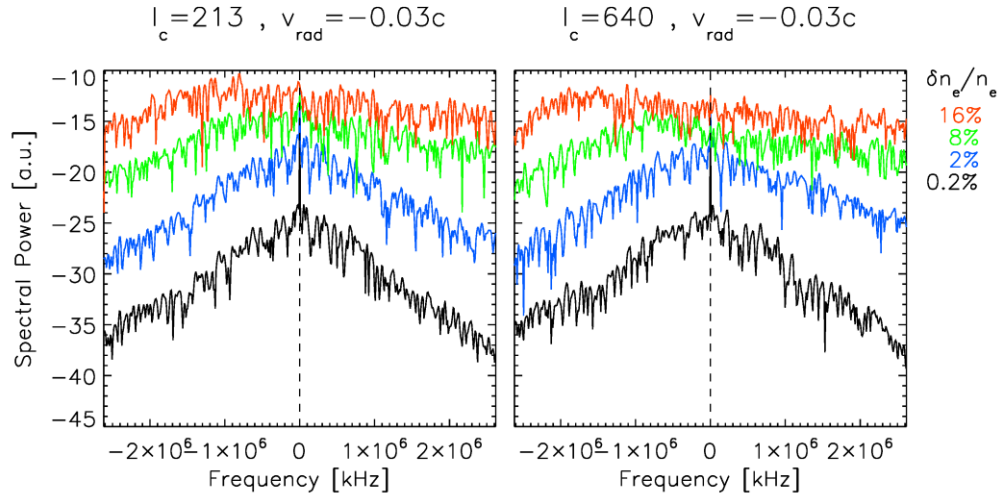


FIG. 5. Power spectra of reflectometry complex amplitude signal  $A(t)e^{i\phi(t)}$  for a set of chosen turbulence levels, where turbulence was generated using a Kolgomorov-like model and set to flow in the radial direction. Spectra are displaced vertically to help visualize the data.

The spectral broadening effect with increasing turbulence levels is again observed. This effect is more intense in this case than for poloidal plasma flow cases, observed previously in figure 1. Equivalently, the phase runaway observed in figure 6, and in particular for the case of shallower gradient, is also more persistent than what was obtained previously with poloidal plasma flow, as shown in figure 3.

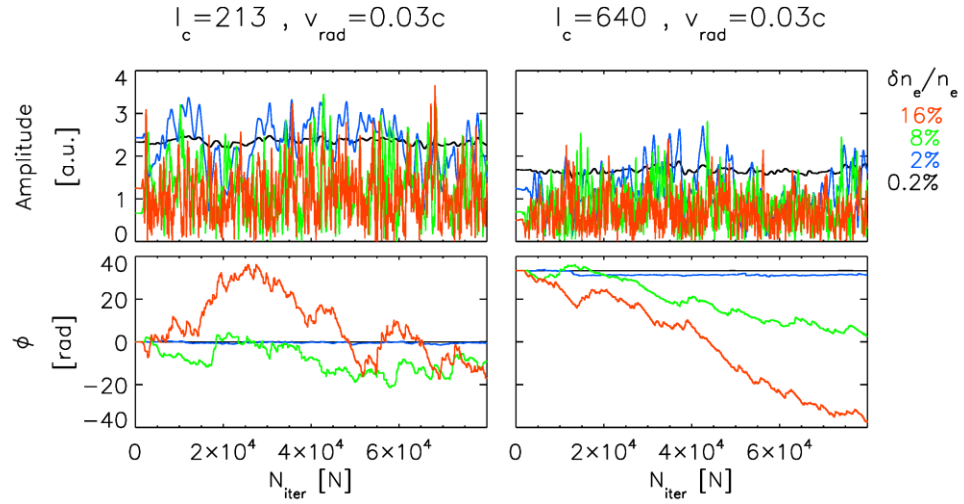


FIG. 6. Evolution of reflectometry amplitude  $A$  and phase  $\phi$  along the time iterations with radial propagation of the turbulence matrix.

The radial flow of turbulent plasmas could induce Doppler effects at both the cutoff location and the Bragg backscattering positions. A single sideband in the frequency spectrum should thus be produced by a density fluctuation with  $k_{\text{rad}} = 2k(r)$  propagating radially. While there is some asymmetry in the complex spectra, it does not allow identifying unarguably the main mechanism leading to the phase runaway. The reduction in the average amplitude with both increasing turbulence levels and density gradient length is again observed.

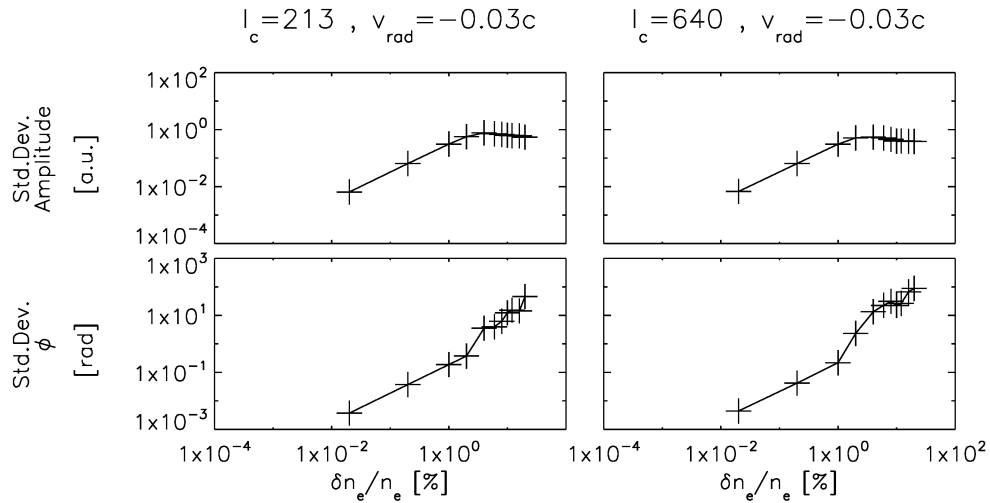


FIG. 7. Standard deviation of the reflectometry amplitude  $A(t)$  and phase  $\phi(t)$  signals against the turbulence level of the Kolgomorov-like turbulent plasmas for a radial plasma flow case, using a log-log plot.

The standard deviation of both the phase and amplitude signals for the full set of simulated turbulence levels are displayed in figure 7. While the linear regime seems to hold only in the low range of  $\delta n_e/n_e$  values, some relation with the phase variations seems to exist even at high density turbulence levels. However, when phase variations become greater than  $\pi$  and the time signals no longer appear to be stationary, a point is reached that may determine the limit to directly extract information about the density fluctuations.

As future work, new simulations with reversed direction of turbulence propagation will be carried out, to check for changes in the sign of dominant phase runaway and, consequently, study the impact of Doppler effects caused by radial movements of both the reflecting layer and of the Bragg backscattering fluctuations. Also, simulations with plasmas obtained from the output of gyro-fluid or gyro-kinetic turbulence codes will be used, to have more realistic plasma models, which can then be benchmarked against the simulation presented here.

## Acknowledgments

This work has been carried out within the framework of the EUROfusion Consortium and has received funding from the Euratom research and training programme 2014-2018 under grant agreement No 633053. IST activities also received financial support from “Fundação para a Ciência e Tecnologia” through project UID/FIS/50010/2013. The views and opinions expressed herein do not necessarily reflect those of the European Commission.

## References

- [1] F. da Silva, S. Heuraux, E. Gusakov and A. Popov, IEEE Trans. Plasma Sci. **38** 2144-8 (2010)
- [2] F. da Silva, S. Heuraux, S. Hacquin and M.E. Manso, Journal of Comp. Physics, **203** 467-92 (2005)
- [3] L. Cupido *et al*, Rev. Sci. Instrum. **77** 10E915 (2006)
- [4] G.D. Conway, L. Schott and A. Hirose, Rev. Sci. Instrum. **67** 3861 (1996)
- [5] S. Heuraux *et al*, Rev. Sci. Instrum. **74**(3) 1501–1505 (2003)
- [6] N. Bretz, Physics of Fluids B: Plasma Physics, **4**(8) 2414–2422 (1992)
- [7] I.H. Hutchinson, Plasma Phys. Control. Fusion, **34**(7) 1225–1251 (1992)

- [8] X.L. Zou, L. Laurent, and J.M. Rax, Plasma Phys. Control. Fusion, **33(8)** 903–918 (1991)
- [9] C. Fanack *et al*, Plasma Phys. Control. Fusion, **38(11)** 1915–1930 (1996)
- [10] I. Boucher *et al*, Plasma Phys. Control. Fusion, **40** 1489-1500 (1998)
- [11] E. Gusakov, S. Heuraux and A. Yu Popov, Plasma Phys. Control. Fusion, **51** 065018 (2009)
- [12] E.V. Sysoeva, E. Gusakov and S. Heuraux, Plasma Phys. Control. Fusion **55**, 115001 (2013)
- [13] G.D. Conway, Plasma Phys. Control. Fusion **41** 65–92 (1999)